Chapter 1
First-Order Optical Systems for Information Processing

Tatiana Alieva
Universidad Complutense de Madrid, Spain

1.1 Introduction

During the last decades, optics is playing an increasingly important role in acquisition, processing, transmission, and archiving of information. In order to underline the contribution of optics in the information acquisition process, let us mention such optical modalities as microscopy, tomography, speckle imaging, spectroscopy, metrology, velocimetry, particle manipulation, etc. Data transmission through optical fibers and optical data storage (CD, DVD, as well as current advances of holographic memories) make us everyday users of optical information technology. In the area of information processing, optics also has certain advantages with respect to electronic computing, thanks to its massive parallelism, operating with continuous data, possibility of direct penetration into the data acquisition process, implementation of fuzzy logic, etc.

The basis of the analog coherent optical information processing is the ability of a thin convergent lens to perform the Fourier transform (FT). More than 40 years ago, Van der Lugt introduced an optical scheme for convolution/correlation operation, based on a cascade of two optical systems performing the Fourier transform with filter mask between them, initiating an era of Fourier optics.[1] This simple scheme realizes the most important shift-invariant operations in signal/image processing, such as filtering and pattern recognition. Nowadays, the Fourier optics area has been expanded with more sophisticated signal processing tools such as wavelets, bilinear distributions, fractional transformations, etc. Nevertheless, the paraxial optical systems (also called first-order or Gaussian ones, which consist for example from several aligned lenses, or mirrors) remain the basic elements for analog optical information processing.

In paraxial approximation of the scalar diffraction theory, a coherent light propagation through such a system is described by a canonical integral transform (CT). Thus starting from the complex field amplitude at the input plane of the system, we have its CT at the output plane. The two-dimensional CTs include, among others, such well-known transformations as image rotation, scaling, fractional Fourier[2] and Fresnel transforms. We can say that the CTs represent a two-dimensional signal in different phase space domains, where the phase space is defined by the position and momentum (spatial frequency) coordinates. The signal manipulation in different phase space domains opens new perspectives for information processing. Indeed, several useful applications of the first-order optical systems for information processing have been proposed in the past decade. In particular first-order optical systems performing fractional Fourier transform have been used for shift-variant filtering, noise reduction, chirp localization, encryption, etc.[2–5] Others have served as mode converters, which transform the

Hermite−Gaussian modes into helicoidal vortex Laguerre−Gaussian ones or other structurally stable modes.[6,7] These modes, in particular, are interesting for new types of information encoding in orbital angular momentum of beam[8] or in the geometric phase accumulated when it undergoes the cyclic transformation.[9]

Moreover the beam evolution in the first-order optical systems is a good model for the analysis of two-dimensional harmonic oscillator.[10]

In this chapter, we briefly summarize the main properties of the two-dimensional CTs,[11] used for the description of the first-order systems, consider their applications to traditional analog optical signal processing tasks, such as filtering, pattern recognition, encryption, etc., and then discuss new methods of information encoding related to the orbital angular momentum transfer and geometric phase accumulation.

1.2 Canonical Integral Transforms: Definition and Classification

1.2.1 Definition

The evolution of the complex field amplitude $f(\boldsymbol{r})$ during its propagation through a first-order optical system is described by the linear integral transform

$$f_o(\boldsymbol{r}_o) = \int_{-\infty}^{\infty} f_i(\boldsymbol{r}_i) K^{\mathbf{t}}(\boldsymbol{r}_i, \boldsymbol{r}_o)\, d\boldsymbol{r}_i,$$

where subindices i and o stand for input and output planes of the system. The kernel $K^{\mathbf{t}}(\boldsymbol{r}_i, \boldsymbol{r}_o)$ is parametrized by the wavelength λ and the real symplectic ray transformation 4×4 matrix $\mathbf{t}$ that relates the position $\boldsymbol{r}_i$ and direction $\boldsymbol{q}_i$ of an incoming ray to the position $\boldsymbol{r}_o$ and direction $\boldsymbol{q}_o$ of the outgoing ray,

$$\begin{bmatrix} \boldsymbol{r}_o \\ \boldsymbol{q}_o \end{bmatrix} = \begin{bmatrix} \mathbf{a} & \mathbf{b} \\ \mathbf{c} & \mathbf{d} \end{bmatrix} \begin{bmatrix} \boldsymbol{r}_i \\ \boldsymbol{q}_i \end{bmatrix} = \mathbf{t} \begin{bmatrix} \boldsymbol{r}_i \\ \boldsymbol{q}_i \end{bmatrix}.$$

Proper normalization of the variables and the matrix parameters to some length factor w and λ leads to the dimensionless variables: $\mathbf{r} = \boldsymbol{r}/\sqrt{\lambda w}$, $\mathbf{q} = \boldsymbol{q}\sqrt{w/\lambda}$, $\mathbf{A} = \mathbf{a}$, $\mathbf{B} = \mathbf{b}/w$, $\mathbf{C} = \mathbf{c}w$, $\mathbf{D} = \mathbf{d}$, which will be used further in this chapter,

$$\begin{bmatrix} \mathbf{r}_o \\ \mathbf{q}_o \end{bmatrix} = \begin{bmatrix} \mathbf{A} & \mathbf{B} \\ \mathbf{C} & \mathbf{D} \end{bmatrix} \begin{bmatrix} \mathbf{r}_i \\ \mathbf{q}_i \end{bmatrix} = \mathbf{T} \begin{bmatrix} \mathbf{r}_i \\ \mathbf{q}_i \end{bmatrix}, \tag{1.1}$$

where $\mathbf{r} = (x, y)^t$ and $\mathbf{q} = (q_x, q_y)^t$. As usual, the superscript ^{t} denotes transposition. The normalized variable $\mathbf{q}$ can also be interpreted as spatial frequency or ray momentum. The canonical integral transform associated with matrix $\mathbf{T}$ will be represented by the operator $\mathcal{R}^{\mathbf{T}}$

$$f_o(\mathbf{r}_o) = \mathcal{R}^{\mathbf{T}}\left[f_i(\mathbf{r}_i)\right](\mathbf{r}_o) = F_{\mathbf{T}}(\mathbf{r}_o) = \int_{-\infty}^{\infty} f_i(\mathbf{r}_i) K^{\mathbf{T}}(\mathbf{r}_i, \mathbf{r}_o)\, d\mathbf{r}_i. \tag{1.2}$$

The CT is a linear transform: $\mathcal{R}^{\mathbf{T}}\left[f(\mathbf{r}_i)+g(\mathbf{r}_i)\right](\mathbf{r}) = \mathcal{R}^{\mathbf{T}}\left[f(\mathbf{r}_i)\right](\mathbf{r}) + \mathcal{R}^{\mathbf{T}}\left[g(\mathbf{r}_i)\right](\mathbf{r})$. It is additive in the sense that $\mathcal{R}^{\mathbf{T}_2}\mathcal{R}^{\mathbf{T}_1} = \mathcal{R}^{\mathbf{T}_2\times\mathbf{T}_1}$. The inverse transformation is parametrized by the matrix $\mathbf{T}^{-1}$, which, because $\mathbf{T}$ is symplectic, is given by

$$\mathbf{T}^{-1} = \begin{bmatrix} \mathbf{D}^t & -\mathbf{B}^t \\ -\mathbf{C}^t & \mathbf{A}^t \end{bmatrix}. \tag{1.3}$$

Any proper normalized symplectic ray transformation matrix can be decomposed in the modified Iwasawa form as[12]

$$\mathbf{T} = \begin{bmatrix} \mathbf{A} & \mathbf{B} \\ \mathbf{C} & \mathbf{D} \end{bmatrix} = \begin{bmatrix} \mathbf{I} & \mathbf{0} \\ -\mathbf{G} & \mathbf{I} \end{bmatrix} \begin{bmatrix} \mathbf{S} & \mathbf{0} \\ \mathbf{0} & \mathbf{S}^{-1} \end{bmatrix} \begin{bmatrix} \mathbf{X} & \mathbf{Y} \\ -\mathbf{Y} & \mathbf{X} \end{bmatrix} = \mathbf{T}_L\mathbf{T}_S\mathbf{T}_O, \tag{1.4}$$

with $\mathbf{I}$ throughout denoting the identity matrix, in which the first matrix represents a lens transform described by the symmetric matrix

$$\mathbf{G} = -(\mathbf{C}\mathbf{A}^t + \mathbf{D}\mathbf{B}^t)(\mathbf{A}\mathbf{A}^t + \mathbf{B}\mathbf{B}^t)^{-1} = \mathbf{G}^t. \tag{1.5}$$

The second matrix corresponds to a scaler described by the positive definite symmetric matrix

$$\mathbf{S} = (\mathbf{A}\mathbf{A}^t + \mathbf{B}\mathbf{B}^t)^{1/2} = \mathbf{S}^t \tag{1.6}$$

and the third is an orthosymplectic[12,13] (i.e., both orthogonal and symplectic) matrix, which can be shortly represented by the unitary matrix

$$\mathbf{U} = \mathbf{X} + i\mathbf{Y} = (\mathbf{A}\mathbf{A}^t + \mathbf{B}\mathbf{B}^t)^{-1/2}(\mathbf{A} + i\mathbf{B}). \tag{1.7}$$

Note that because $\mathbf{A} = \mathbf{S}\mathbf{X}$ and $\mathbf{B} = \mathbf{S}\mathbf{Y}$, the products $\mathbf{B}^{-1}\mathbf{A} = \mathbf{Y}^{-1}\mathbf{X}$ and $\mathbf{A}^{-1}\mathbf{B} = \mathbf{X}^{-1}\mathbf{Y}$ used further in different relations are defined by the orthogonal matrix $\mathbf{T}_O$.

Because the ray transformation matrix $\mathbf{T}$ is symplectic and therefore

$$\begin{aligned} &\mathbf{A}\mathbf{B}^t = \mathbf{B}\mathbf{A}^t, \quad \mathbf{C}\mathbf{D}^t = \mathbf{D}\mathbf{C}^t, \quad \mathbf{A}\mathbf{D}^t - \mathbf{B}\mathbf{C}^t = \mathbf{I}, \\ &\mathbf{A}^t\mathbf{C} = \mathbf{C}^t\mathbf{A}, \quad \mathbf{B}^t\mathbf{D} = \mathbf{D}^t\mathbf{B}, \quad \mathbf{A}^t\mathbf{D} - \mathbf{C}^t\mathbf{B} = \mathbf{I}, \end{aligned} \tag{1.8}$$

it has only ten free parameters. We call the transform associated with $\mathbf{T}$ *separable* if the block matrices $\mathbf{A}$, $\mathbf{B}$, $\mathbf{C}$, and $\mathbf{D}$ and $\mathbf{G}$, $\mathbf{S}$, $\mathbf{X}$, and $\mathbf{Y}$ correspondingly are diagonal. A separable transform has six degrees of freedom which reduce to three for rotational symmetric case corresponding to scalar block matrices.

In the often-used case $\det \mathbf{B} \neq 0$, the CT takes the form of Collins' integral[14]

$$\begin{aligned} f_o(\mathbf{r}_o) = \mathcal{R}^{\mathbf{T}}\left[f_i(\mathbf{r}_i)\right](\mathbf{r}_o) = (\det i\mathbf{B})^{-1/2} \int_{-\infty}^{\infty} f_i(\mathbf{r}_i) \\ \times \exp\left[i\pi\left(\mathbf{r}_i^t\mathbf{B}^{-1}\mathbf{A}\mathbf{r}_i - 2\mathbf{r}_i^t\mathbf{B}^{-1}\mathbf{r}_o + \mathbf{r}_o^t\mathbf{D}\mathbf{B}^{-1}\mathbf{r}_o\right)\right] \mathrm{d}\mathbf{r}_i. \end{aligned} \tag{1.9}$$

The kernel corresponds to two-dimensional generalized chirp function because its phase is a polynomial of second degree of variables $\mathbf{r}_i$ and $\mathbf{r}_o$. In particular

Chapter 11
Digital Computational Imaging

Leonid Yaroslavsky
Tel Aviv University, Israel

11.1 Introduction: Present-Day Trends in Imaging

Imaging has always been the primary goal of informational optics. The whole history of optics is, without any exaggeration, a history of creating and perfecting imaging devices. Starting more than 2000 years ago from ancient magnifying glasses, optics has been evolving with ever increasing speed from Galileo’s telescope and van Leeuwenhoek’s microscope, through mastering new types of radiations and sensors, to the modern wide variety of imaging methods and devices of which most significant are holography, methods of computed tomography, adaptive optics, synthetic aperture and coded aperture imaging, and digital holography. The main characteristic feature of this latest stage of the evolution of optics is integration of physical optics with digital computers. With this, informational optics is reaching its maturity. It is becoming digital and imaging is becoming computational.

The following qualities make digital computational imaging an ultimate solution for imaging:

- Processing versatility. Digital computers integrated into optical information processing and imaging systems enable them to perform not only element wise and integral signal transformations such as spatial Fourier analysis,

signal convolution, and correlation, which are characteristic for analog optics, but any operations needed. This eliminates the major limitation of optical information processing and makes optical information processing integrated with digital signal processing almost almighty.

- Flexibility and adaptability. No hardware modifications are necessary to reprogram digital computers for solving different tasks. With the same hardware, one can build an arbitrary problem solver by simply selecting or designing an appropriate code for the computer. This feature makes digital computers also an ideal vehicle for processing optical signals adaptively since, with the help of computers, they can easily be adapted to varying signals, tasks, and end-user requirements.
- Universal digital form of the data. Acquiring and processing quantitative information carried by optical signals and connecting optical systems to other informational systems and networks is most natural when data are handled in a digital form. In the same way that in economics money is a general equivalent, digital signals are the general equivalent in information handling. Thanks to its universal nature, the digital signal is an ideal means for integrating different informational systems.

Present-day main trends in digital computational imaging are as follows:

- Development and implementation of new digital image acquisition, image formation, and image display methods and devices
- Transition from digital image processing to real-time digital video processing
- Widening the front of research toward 3D imaging and 3D video communication

Currently there is a tremendous amount of literature on digital computational imaging, which is impossible to comprehensively review here, and the present-day trends can only be illustrated on some examples. In this chapter, we use an example of three developments, in which the present author was directly involved. In Section 11.2 we describe a new family of image sensors that are free of diffraction limitations of conventional lens-based image sensors and base their image formation capability solely on numerical processing of radiation intensity measurements made by a set of simple radiation sensors with natural cosine law spatial sensitivity. In Section 11.3 we describe real-time digital video processing for perfecting visual quality of video streams distorted by camera noise and atmospheric turbulence. For the latter case, the processing not only produces good quality video for visual analysis, but in addition, makes use of atmospheric turbulence-induced image instabilities to achieve image super-resolution beyond the limits defined by the camera sampling rate. In Section 11.4 we present a computer-generated display hologram based 3D video communication paradigm.

11.2 Opticsless Imaging Using "Smart" Sensors

One can treat images as data that indicate location in space and intensities of sources of radiation. In conventional optical imaging systems, the task of determining positions of sources of light is solved by lenses, and the task of measurement of light source intensities is solved by light-sensitive plane sensors such as photographic films or CCD/CMOS electronic sensor arrays. A lens directs light from each of the light sources to a corresponding place on the sensor plane, and the intensity sensor's output signal at this place provides an estimate of the light source intensity.

Lenses are wonderful processors of directional information carried by light rays. They work in parallel with all light sources in their field of view and with the speed of light. However, their high perfection has its price. Light propagation from the lens to the sensor's plane is governed by the diffraction laws. They limit the capability of the optical imaging system to distinguish light radiated from different light sources and to discriminate closely spaced sources. According to the theory of diffraction, this capability, called imaging system resolving power, is determined by the ratio of the light wavelength times the lens's focal distance and the dimensions of the lens. Therefore, good imaging lenses are large and heavy. Perfect lenses that produce low aberrations are also very costly. In addition, lens-based imaging systems have limited field of view and lenses are not available for many practically important kinds of radiation such as, for instance, x-rays and radioactive radiation. This motivates search for optics-less imaging devices.

Recently, H. J. Caulfield and the present author suggested a concept of a new family of opticsless radiation sensors[1,2] that exploits the idea of combining the natural cosine law directional sensitivity of radiation sensors with the computational power of modern computers and digital processors to secure the sensor's spatial selectivity required for imaging. These opticsless "smart" (OLS) sensors consist of an array of small elementary subsensors with the cosine law angular selectivity supplemented with a signal processing unit (the sensor's "brain") that processes the subsensors' output signals to produce maximum likelihood (ML) estimates of spatial locations of radiation sources and their intensities.

Two examples of possible designs of the OLS sensors are sketched in Fig. 11.1. Figure 11.1(a) shows an array of elementary subsensors arranged on a curved surface, such as spherical one. Such an array of subsensors, together with its signal processing unit, is capable of localizing sources of radiation and measuring their intensities at any distances and in a 4π steradian solid angle. Shown in Fig. 11.1(b) is an array of elementary subsensors on a flat surface together with its signal processing unit that is capable of measuring coordinates and intensities of radiation sources at close distances.

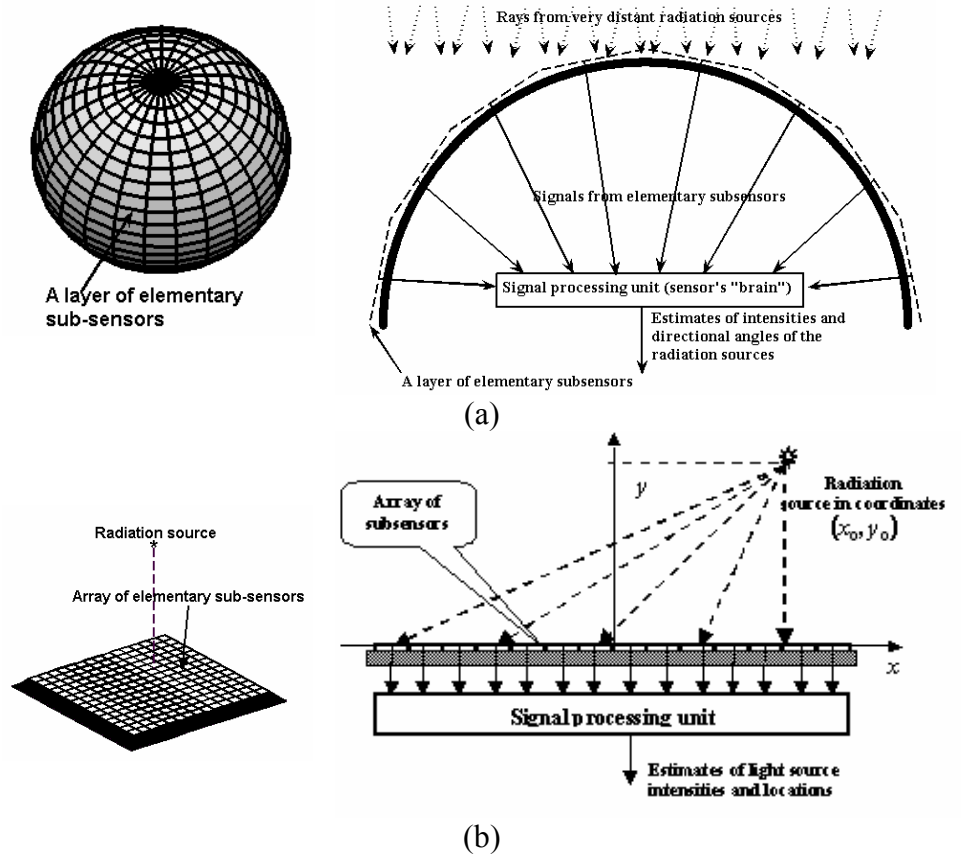

Figure 11.1 Two examples of possible designs of opticsless "smart" radiation sensors and their corresponding schematic diagrams.

The work principle of opticsless smart sensors can be explained using a simple special case of locating a certain number K of very distant radiation sources by an array of N elementary sensors placed on a curved surface. Consider a 1D model of sensor's geometry sketched in Fig. 11.2. For an nth elementary sensor with the cosine law spatial selectivity placed at angle φ_n with respect to the sensor's "optical" axis, its output signal $s_{n,k}$ to a ray of light emanating from the kth source under angle θ_k with respect to the sensor's "optical" axis is proportional to the radiation intensity I_k and cosine of angle $\theta_{n,k}$ between the vector of electrical field of the ray and the normal to the elementary sensor surface. Additionally, this signal contains a random component ν_n that describes the subsensor's immanent noise as

$$s_n = A_k \overline{\cos}\theta_{n,k} + \nu_n = A_k \overline{\sin}\left(\varphi_n + \theta_k\right) + \nu_n \,, \tag{11.1}$$

Chapter 27

Strongly Correlated Quantum Phases of Ultracold Atoms in Optical Lattices

Immanuel Bloch
Johannes Gutenberg-Universität, Germany

27.1 Introduction

Ultracold quantum gases in optical lattices form almost ideal conditions to analyze the physics of strongly correlated quantum phases in periodic potentials. Such strongly correlated quantum phases are of fundamental interest in condensed matter physics, because they lie at the heart of topical quantum materials, such as high-T_c superconductors and quantum magnets, which pose a challenge to our basic understanding of interacting many-body systems. Quite generally, such strongly interacting quantum phases arise when the interaction energy between two particles dominates over the kinetic energy of the two particles. Such a regime can either be achieved by increasing the interaction strength between the atoms via Feshbach resonances or by decreasing the kinetic energy, such that eventually the interaction

energy is the largest energy scale in the system. The latter can, for example, simply be achieved by increasing the optical lattice depth.

This chapter tries gives an introduction into the field of optical lattices and the physics of strongly interacting quantum phases. A prominent example hereof is the superfluid-to-Mott insulator transition,[1–5] which transforms a weakly interacting quantum gas into a strongly correlated many body system. Dominating interactions between the particles are in fact crucial for the Mott insulator transition and also for the realization of controlled interaction-based quantum gates,[6–8] of which several have been successfully realized experimentally.[9–11]

27.2 Optical Lattices

27.2.1 Optical dipole force

In the interaction of atoms with coherent light fields, two fundamental forces arise.[12,13] The so-called Doppler force is dissipative in nature and can be used to efficiently laser cool a gas of atoms and relies on the radiation pressure together with spontaneous emission. The so-called dipole force, on the other hand, creates a purely conservative potential in which the atoms can move. No cooling can be realized with this dipole force; however, if the atoms are cold enough initially, then they may be trapped in such a purely optical potential.[14,15]

How does this dipole force arise? We may grasp the essential points through a simple classical model in which we view the electron as harmonically bound to the nucleus with oscillation frequency ω_0. An external oscillating electric field of a laser $\mathbf{E}$ with frequency ω_L can now induce an oscillation of the electron resulting in an oscillating dipole moment $\mathbf{d}$ of the atom. Such an oscillating dipole moment will be in phase with the driving oscillating electric field, for frequencies much lower than an atomic resonance frequency and 180 deg out of phase for frequencies much larger than the atomic resonance frequency. The induced dipole moment again interacts with the external oscillating electric field, resulting in a dipole potential V_{dip} experienced by the atom[15–19]

$$V_{dip} = -\frac{1}{2}\langle \mathbf{dE} \rangle, \tag{27.1}$$

where $\langle \cdot \rangle$ denotes a time average over fast oscillating terms at optical frequencies. From Eq. (27.1) it becomes immediately clear that for a red detuning ($\omega_L < \omega_0$), where $\mathbf{d}$ is in phase with $\mathbf{E}$, the potential is attractive, whereas for a blue detuning ($\omega_L > \omega_0$), where $\mathbf{d}$ is 180 deg out of phase with $\mathbf{E}$, the potential is repulsive. By relating the dipole moment to the polarizability $\alpha(\omega_L)$ of an atom and expressing the electric field amplitude E_0 via the intensity of the laser field I, one obtains for the dipole potential

$$V_{dip}(\mathbf{r}) = -\frac{1}{2\epsilon_0 c}\mathrm{Re}(\alpha) I(\mathbf{r}). \tag{27.2}$$

A spatially dependent intensity profile $I(\mathbf{r})$ can therefore create a trapping potential for neutral atoms.

For a two-level atom a more useful form of the dipole potential may be derived within the rotating wave approximation, which is a reasonable approximation provided that the detuning $\Delta = \omega_L - \omega_0$ of the laser field ω_L from an atomic transition frequency ω_0 is small compared to the transitions frequency itself, $\Delta \ll \omega_0$. Here, one obtains[15]

$$V_{dip}(\mathbf{r}) = \frac{3\pi c^2}{2\omega_0^3}\frac{\Gamma}{\Delta} I(\mathbf{r}), \tag{27.3}$$

with Γ being the decay rate of the excited state. Here, a red- detuned laser beam ($\omega_L < \omega_0$) leads to an attractive dipole potential and a blue-detuned laser beam ($\omega_L > \omega_0$) leads to a repulsive dipole potential. By simply focusing a Gaussian laser beam, this can be used to attract or repel atoms from an intensity maximum in space (see Fig. 27.1).

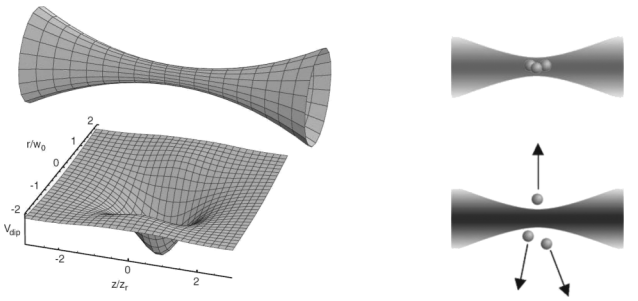

Figure 27.1 (a) Gaussian laser beam together with corresponding trapping potential for a red-detuned laser beam. (b) A red- detuned laser beams leads to an attractive dipole potential, whereas a blue detuned laser beam leads to a repulsive potential (c).

For such a focused gaussian laser beam, the intensity profile $I(r, z)$ is given by

$$I(r, z) = \frac{2P}{\pi w^2(z)} e^{-2r^2/w^2(z)}, \tag{27.4}$$

where $w(z) = w_0(1 + z^2/z_R^2)$ is the $1/e^2$ radius, depending on the z coordinate, $z_R = \pi w^2/\lambda$ is the Rayleigh length and P is the total power of the laser beam.[20] Around the intensity maximum a potential depth minimum occurs for a red-detuned laser beam, leading to an approximately harmonic potential of the form

$$V_{dip}(r, z) \approx -V_0 \left[1 - 2\left(\frac{r}{w_0}\right)^2 - \left(\frac{z}{z_R}\right)^2\right]. \tag{27.5}$$

This harmonic confinement is characterized by radial ω_r and axial ω_{ax} trapping frequencies $\omega_r = (4V_0/mw_0^2)^{1/2}$ and $\omega_z = (2V_0/mz_R^2)$.